Laminar Forced Convective Heat Transfer in Rectangular Cavity with Three Heated Blocks and Attached Baffle

Faris Ali Badawy
Asst. Lecturer
Department of Mechanical Power
Institute of Technology
Middle Technical University
Baghdad\ Iraq
Email: faris_alzubady@yahoo.com

Abstract :-

The laminar forced convective heat transfer in rectangular cavity with three heated blocks subjected to constant heat flux at bottom wall. A single baffle was attached to the top wall. A steady, incompressible, and laminar flow assumption was adopted to solve a numerical of two-dimensional cavity mode. The finite volumes approach was used to solve the governing equations and employed the SIMPLE algorithm on the collocated arrangement. The numerical simulation was performed at different cavity aspect ratios L/H (3.2, 3.8, 4.5, and 5.6), different baffle height ratio h/H (0, 0.2, 0.3, and 0.4) and different block height given ratio b/H (0.2, 0.4, 0.5, and 0.8). The air inlet to the cavity with at various Raleigh number (8.2×10^6 to 4.9×10^7) and Richardson number at (1.3, 2.1, 3.6, and 8.2). In addition, to study the effect of using the forced convection heat transfer the Reynolds number was varied as (1100, 1170, 1900, and 2100). The results of the flow and temperature distributions and Nusselt numbers were presented. The results showed that the velocity and temperatures were affected by the flow and geometrical conditions of the cavity. Also, the results predicted that the Nusselt number increased with increasing Reynolds number, baffle height ratio and box height ratio but it decreased with increasing the cavity aspect ratio in all studied conditions.

Keywords: Baffle, Heated Blocks, Laminar Forced Convection, Cavity.

1. Introduction

The airflow due to the convection in enclosures and cavities has been a subject of interest for many years due to their ever-increasing applications in electronic cooling, solar collectors, lubrication technologies, nuclear reactors, and food processing. The phenomenon of convection heat transfer is called mixed convection when both modes of natural and forced convections simultaneously exist. When its buoyant flow matters in a forced flow or when the effect of forced flow matters in a buoyant flow, the mixed convection heat transfer was occurred. Several dimensionless numbers such as: Grashof number (Gr), Reynolds number (Re), Rayleigh number (Ra), Prandtl number (Pr) and Richardson number (Ri) which are used to determine the type of flow. So, the dividing natural convection effect by forced convection effect represented by Richardson number [1]. The mixed convection in square cavities with two moving walls was studied numerically by [2]. Their results showed that the heat transfer decreases significantly with vertical walls moving upwards in the same direction. Also, the numerical study of the trapezoidal cavities for natural convection with two baffles attached on the lower surface was presented by [3]. They were examined a cavity whose lower and upper are both adiabatic while the vertical walls are isothermal to assess the effects of the baffle's height. Their results showed that the second baffle decreases the cavity's fluid flow and heat transfer. In addition, the heat transfer drops drastically as the height of the baffle rises. However, a numerical study on the mixed convection in a lid driven cavity with a heated square blockage was studied in [4]. Their results showed that the average Nusselt number of heater significantly affected by the size, location and Richardson number of the heater eccentricities. The convection in trapezoidal cavities, especially those with two internal baffles attracted on the top surface, an insulated floor and isothermal left-heated and isothermal right-cooled vertical walls was examined by [5]. A parametric study was performed for a wide range of Rayleigh numbers ($10^3 < Ra < 10^6$) baffle heights ratio given by ($H/3$, $2H/3$, and $H/$) where H represent the cavity height, Prandtl numbers given by (0.7, 10 and 130). Moreover, the problem of the mixed convection in a vented cavity with a centered heat-generating element was studied by [6]. They found that the studied parameters such as Hartmann number, Prandtl number and Reynolds number play a significant role on both the flow and thermal field.

As showing above, there is a few efforts has been given to study the laminar forced convective heat transfer problem in cavities with three heated blocks in bottom surface. Thus,

the aim of this study is to explore the heat transfer rate by laminar convective heat transfer in a cavity with three heated blocks as in the brick industry. The present work is studied the effects of height of the three heating blocks and the height of the baffle inside a rectangular cavity on the heat transfer and fluid flow.

2. Mathematical model

The geometry description of the 2D rectangular cavity was presented in the **Fig.1**. The cavity consists of top wall is equipped with a vertical baffle with constant thickness of (3 mm) and variable height (h). The bottom wall has three blocks has a constant pitch between them of (5 mm) with variable height (b) and applied constant heat flux. The left and right walls are equipped with an air inlet and air outlet ports with constant height of (5 mm).

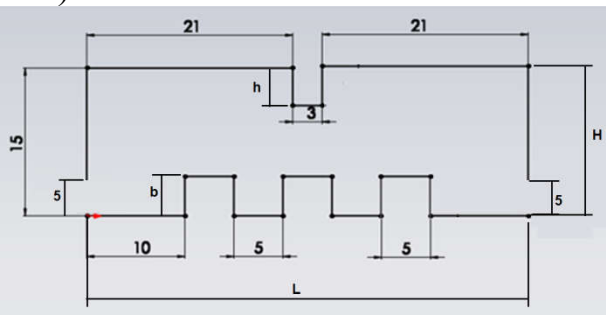

Fig.1 Dimensions of the present cavity (all dimensions in mm).

By considering the air motion within a rectangular cavity with right and left insulated walls with variable height (H) and the top and bottom insulated walls with constant length (L) that it was assumed heated by a constant heat flux (q'') as shown in **Fig.2**.

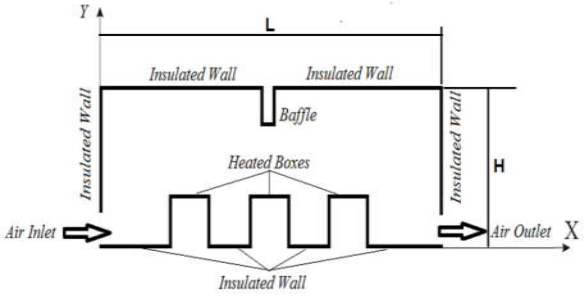

Fig.2 Schematic diagram of the physical system

The fluid properties are assumed constant except for the density variation that is treated according to Boussinesq approximation. The present flow is considered steady, laminar, incompressible and two-dimensional [7]. The viscous incompressible flow and the temperature distribution inside the cavity are described by the Navier–Stokes and the energy equations, respectively [8]:

Continuity equation:

$$\frac{\partial u}{\partial x}+\frac{\partial v}{\partial y}=0 \quad (1)$$

x- component of momentum equation:

$$u\frac{\partial u}{\partial x}+v\frac{\partial u}{\partial y}=-\frac{1}{\rho}\frac{\partial \mathrm{p}}{\partial x}+v\left[\frac{\partial^2 u}{\partial x^2}+\frac{\partial^2 u}{\partial y^2}\right] \quad (2)$$

y- component of momentum equation:

$$u\frac{\partial v}{\partial x}+v\frac{\partial v}{\partial y}=-\frac{1}{\rho}\frac{\partial p}{\partial y}+\nu\left[\frac{\partial^2 v}{\partial x^2}+\frac{\partial^2 v}{\partial y^2}\right]+g\beta(T-T_C)$$

(3)

The energy equation:

$$u\frac{\partial T}{\partial x}+v\frac{\partial T}{\partial y}=\alpha\left[\frac{\partial^2 T}{\partial x^2}+\frac{\partial^2 T}{\partial y^2}\right] \qquad (4)$$

The variables of non-dimensional are defined as:

$$X=\frac{x}{L},Y=\frac{y}{L},U=\frac{u}{u_i},V=\frac{v}{u_i},P=\frac{p}{\rho u^2{}_i},\theta=\frac{T-T_i}{T_h-T_i},\theta=\frac{T_s-T_i}{T_h-T_i}$$

And the dimensionless parameters of Re, Ri, Pr and K are defined as [8]:

$$\mathrm{Re}=\frac{u_i E}{\nu},Ri=\frac{g\beta(T-T_i)E}{u_i^2},\mathrm{Pr}=\frac{\nu}{\alpha}$$

Using dimensionless parameters variables defined above, the non-dimensional forms of the governing equations of the present problem are obtained as follows [8]:

Dimensionless continuity equation:

$$\frac{\partial U}{\partial X}+\frac{\partial V}{\partial Y}=0$$

(5)

Dimensionless x- component of momentum equation:

$$U\frac{\partial U}{\partial X}+V\frac{\partial U}{\partial Y}=-\frac{\partial P}{\partial X}+\frac{1}{\mathrm{Re}}\left[\frac{\partial^2 U}{\partial X^2}+\frac{\partial^2 U}{\partial Y^2}\right]$$

(6)

Dimensionless y- component of momentum equation:

$$U\frac{\partial V}{\partial X}+V\frac{\partial V}{\partial Y}=-\frac{\partial P}{\partial Y}+\frac{1}{\mathrm{Re}}\left[\frac{\partial^2 V}{\partial X^2}+\frac{\partial^2 V}{\partial Y^2}\right]+Ri\theta$$

(7)

The energy equation:

$$U\frac{\partial T}{\partial X}+V\frac{\partial T}{\partial Y}=\frac{1}{\mathrm{Re}\,\mathrm{Pr}}\left[\frac{\partial^2 \theta}{\partial X^2}+\frac{\partial^2 \theta}{\partial Y^2}\right]$$

(8)

The appropriate dimensionless form of the boundary conditions summarized by **Fig.3** used to solve equations (5) to (8) inside the cavity is given as:

At the inlet;

U=1, V=0, $\theta=\theta_i$

Boundary condition at the outlet:

P=0

At all wall boundaries:

U=0, V=0, $\frac{\partial P}{\partial n}=0$

At the heated blocks wall:

θ=1

At the left, top and bottom walls:

$$\left.\frac{\partial \theta}{\partial X}\right|_{X=0}=\left.\frac{\partial \theta}{\partial Y}\right|_{Y=1,0}$$

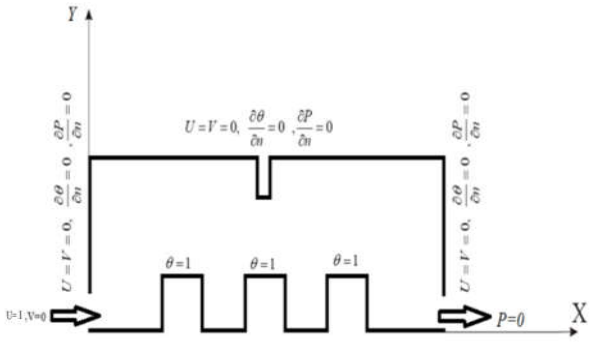

Fig.3. Schematic Diagram of the Boundary Conditions

At the heated wall, the average Nusselt number (Nu) is defined as**:**

$$Nu = \frac{1}{H}\int_0^H \left.\frac{\partial\theta}{\partial X}\right|_{X=1} dY \qquad (9)$$

And the bulk average temperature in the cavity is defined as:

$$\theta_{av} = \int_0^H \frac{1}{\bar{V}}\theta\, d\bar{V} \qquad (10)$$

4. Numerical Technique

In this study, finite volume method was considered to discretization the above governing equations. Using the implicit line by line Gause elimination scheme, the discretization equations is transformed the system of elliptic partial differential equations into a system of algebraic equations. A computer program FORTRAN is used to attain the results using the pressure velocity coupling SIMPLE (Semi-Implicit Method for Pressure Linked Equations) is used to solve the coupled pressure– velocity equation while Hybrid Differencing Scheme (HDS) of [9]. This is the essence of the SIMPLE procedure. The SIMPLE assume **Fig.4a** that Patankar [7]:

$$p = p^* + p' \qquad (11)$$

$$u = u^* + u' \qquad (12)$$

$$v = v^* + v' \qquad (13)$$

where the asterisk represents a guessed value and the prime is the correction necessary to satisfy continuity. The discretization equations for the guessed velocities are then [7]:

$$a_e u_e^* = \sum_i a_i u_i^* + c + \Delta A_e (P_P^* - P_E^*) \qquad (14)$$

$$a_n v_n^* = \sum_i a_i v_i^* + c + \Delta A_n (P_P^* - P_N^*) \qquad (15)$$

from equations (14 and 15) we get:

$$a_e u_e' = \sum_i a_i u_i' + \Delta A_e (P_P' - P_E') \qquad (16)$$

$$a_n v_n' = \sum_i a_i v_i' + \Delta A_n (P_P' - P_N') \qquad (17)$$

for computational convenience, $\sum_i a_i u_i'$, $\sum_i a_i v_i'$, and $\sum_i a_i w_i'$ are set to zero, we get:

$$u_e' = (\Delta A_e / a_e)(P_P' - P_E') \qquad (18)$$

$$v_n' = (\Delta A_n / a_n)(P_P' - P_N') \qquad (19)$$

which is the velocity correction formula and can be written for all the three components as[7]:

$$u_e = u_e^* + (\Delta A_e / a_e)(P_P' - P_E') \qquad (20)$$

$$v_n = v_n^* + (\Delta A_n / a_n)(P_P' - P_N') \qquad (21)$$

If we can now substitute the velocity components given in equations (20 and 21) into the discretized continuity equation (22) written as[7]:

$$F_e - F_w + F_n - F_s = 0 \qquad (22)$$

Rearrange the terms, the following discretization equation for pressure correction is obtained:

$$\sum_i a_i p_p{}' = \sum_i a_i p_i{}' + c \qquad (23)$$

where

$$\sum_i a_i = a_E + a_W + a_N + a_S$$

$$\sum_i a_i p_i{}' = a_E p_E{}' + a_W p_W{}' + a_N p_N{}' + a_S p_S$$

$$a_E = (\rho_e / a_e)(\Delta A_e)^2 \quad ,$$

$$a_W = (\rho_w / a_w)(\Delta A_w)^2$$

$$a_N = (\rho_n / a_n)(\Delta A_n)^2 \quad ,$$

$$a_S = (\rho_s / a_s)(\Delta A_s)^2$$

$$c = F_w{}^* - F_e{}^* + F_s{}^* - F_n{}^*$$

$$F_w{}^* = (\rho u^*)_w \Delta A_w,$$

$$F_e{}^* = (\rho u^*)_e \Delta A_e$$

$$F_s{}^* = (\rho u^*)_s \Delta A_s,$$

$$F_n{}^* = (\rho u^*)_n \Delta A_n$$

The relaxation factors used for velocity components, temperature, and pressure, which adjusted for each case, studied in order to accelerate convergence given by 0.3, 0.6 and 0.8 respectively. The region near the walls, the uniform grid with refinements is used. The computational grids are presented in **Fig.4b**. The model is terminated when the mass, momentum, and energy for each simulation evaluated over the course, residuals drop below 10^{-7}. Moreover, in these numerical simulations, the convergence criterion for temperature, pressure, and velocity is [10]:

$$Error = \frac{\sum_{k=1}^{l}\sum_{i=1}^{m}\sum_{j=1}^{n}|\xi_{i,j,k}^{t+1} - \xi_{i,j,k}^{t}|}{\sum_{k=1}^{l}\sum_{i=1}^{m}\sum_{j=1}^{n}|\xi_{i,j,k}^{t+1}|} \leq 10^{-7} \qquad (24)$$

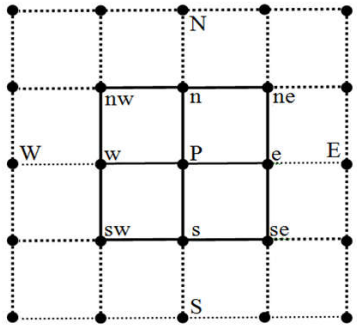

(a)

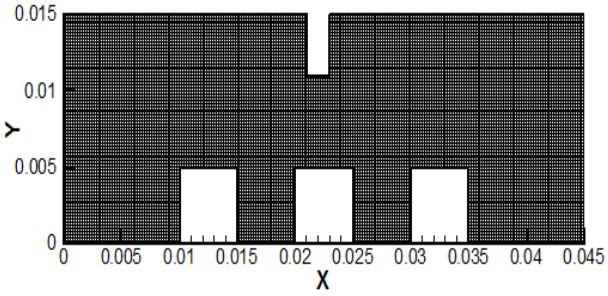

(b)

Fig.4 (a) Location of variables and associated control volumes of (x-y) plane, (b) Meshed computational domain.

4.1 Grid Independent Test

Before conducting the simulation, the computational domain presented in above is tested for grid independence test for better result accuracy as well as time effectiveness. In the present work, four different mesh size models were modeled using Design Modular and only one suitable mesh will be selected for simulation model. The model with very fines mesh size will be taken as reference for the other models. To make sure that the results are due to the boundary conditions and physics used, not the mesh

resolution, mesh independence should be studied in CFD. If the results do not change appreciably, the original grid is probably adequate. Computations have carried out for four selected node sizes (i.e., 5612, 6807, 9789 and 14968).

Table.1 presented grid independence summary of the test results. The results showed that the nodes given at 9789 and 14968 produce almost identical results with a percentage error of 0.02%. Thus, a computational domain with nodes of 14968 was chosen to increase the computational accuracy.

Table.1 Grid independent test

Mesh Type	Number of Nodes	Heated wall maximum Nusselt number	Difference with previous coarse mesh (%)
Course	5612	25.36546	Reference
Medium	6807	26.28847	3.2 %
Fine	9789	27.02515	2.7 %
Very Fine	14968	27.52786	1.8 %

3. Results and Discussion

The present numerical results carried out for 2D laminar forced convective heat transfer and fluid flow in a rectangular cavity with three blocks fixed in the bottom wall but a vertical baffle attached in the top wall. The results presented by distribution of convective velocity, isotherm temperatures contours, local and average Nusselt numbers.

The effect of inlet Reynolds and Raleigh number on the distribution of x-velocity and isotherm contours for values of L/H=4.5, h/H=0.2 and b/H=0.4 is depicted in **Figs.5 to 8.** Generally**,** in the region between the baffle and the heated blocks in the middle region of the cavity, it showed that the velocity increases due to decreasing the cross section area of the airflow. However, in the same time the air velocity decreased in the zones that behind the baffle and in the zones between the heated block. Also, it can be note that the flow creates a cell of recirculation zone in these zones due to the reversed air flow, the intensity of these cells depended on the Reynolds number, so as the Reynolds number increased the cell velocity will increase too.

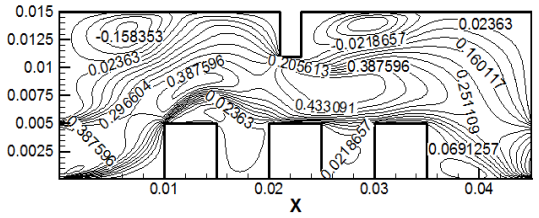

a) Re= 1100

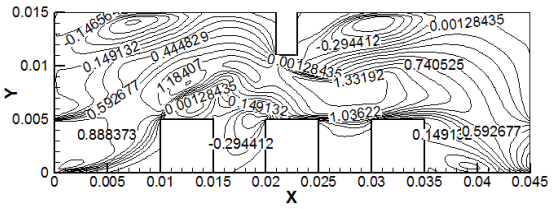

b) Re= 2100

Fig.5 Velocity line distribution variation with Reynolds number at Ra= 8.7×10^6 and Ri=1.3, L/H=4.5, h/H=0.2 and b/H=0.4.

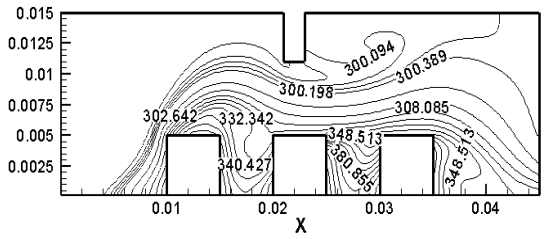

a) Re= 1100

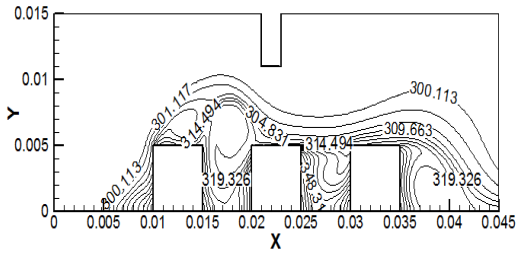

b) Re= 2100

Fig.6 Temperatures distribution variation with Reynolds number at Ra= 1.7×10^6 and Ri=1.3, L/H=4.5, h/H=0.2 and b/H=0.4.

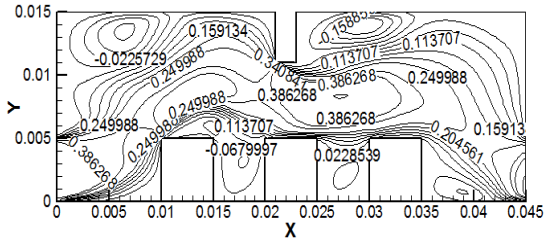

a) Ra= 1.7×10^6

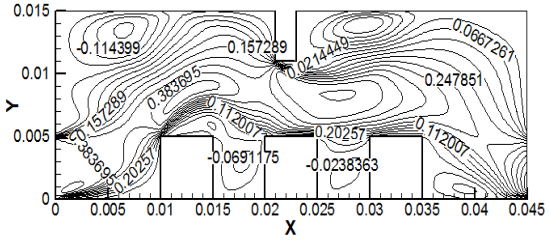

b) Ra= 5.2×10^7

Fig.7 Velocity line distribution variation with Raleigh number at Ri=8.2, L/H=4.5, h/H=0.2 and b/H=0.4.

The distribution of the isotherm temperatures contours will become more stratified to the heated blocks as the Raleigh number increased as show in **Fig. 8**.

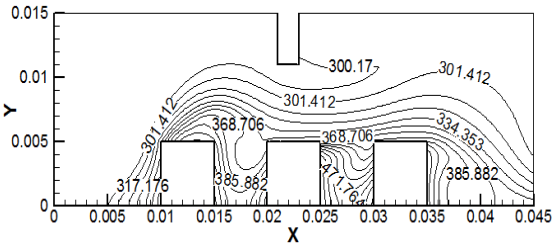

a) Ra= 1.7×10^6

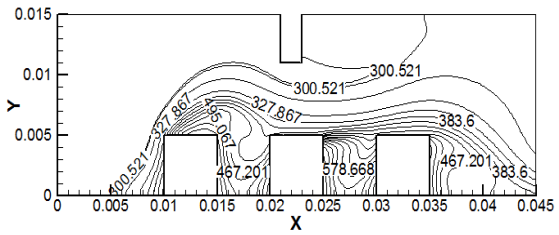

b) Ra= 5.2×10^7

Fig.8 Temperature line distribution variation with Raleigh number at Ri=8.2, L/H=4.5, h/H=0.2 and b/H=0.4.

Baffle height ratio h/H has significant influence on the-velocity and isotherm contours of the airflow in cavity as presented in **Figs.9 and 10**. The results indicated that the increasing the baffle height ratio will lead to increase the velocity under the baffle and will increase the intensity and size behind the baffle.

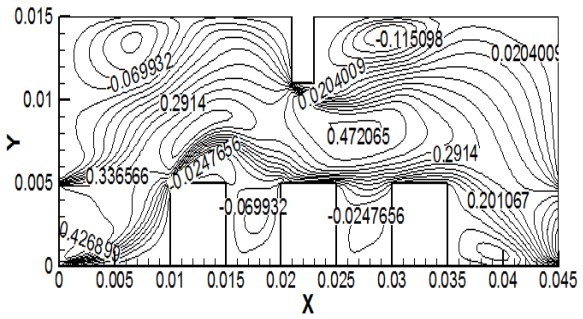

a) h/H=0.2

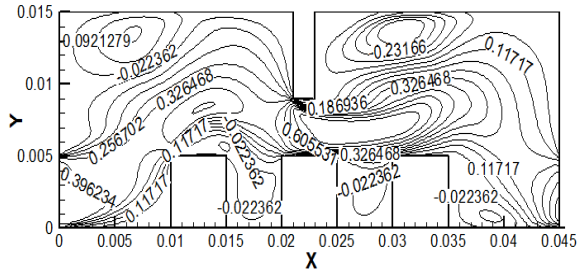

b) h/H=0.4

Fig.9 Velocity line distribution variation with baffle height at Ra= 1.7×10⁶ and Ri=1.3, L/H=4.5 and b/H=0.4

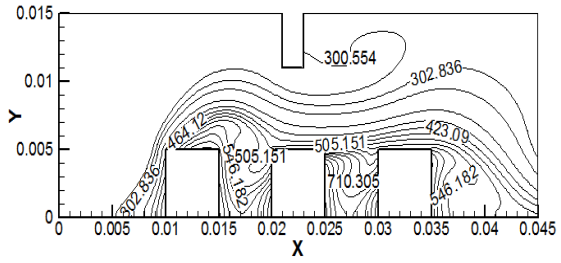

a) h/H=0.2

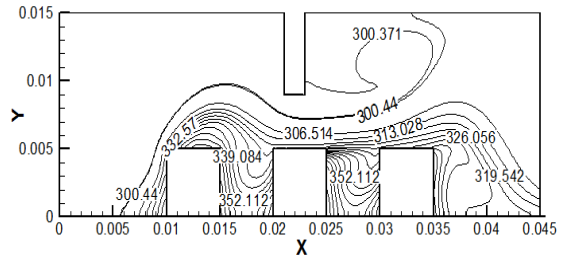

b) h/H=0.4

Fig.10 Velocity line distribution variation with baffle height at Ra= 1.7×10⁶ and Ri=1.3, L/H=4.5 and b/H=0.4.

In addition, when increasing the baffle height ratio the isotherm contours inside the region that between the heated blocks will become more stratified near the blocks and this help to decreasing the air temperatures in these regions. However increasing the aspect ratio L/H of the cavity will decrease the velocity values under the baffle region due to increase the cross section of the airflow, as plotted in **Fig.11.**

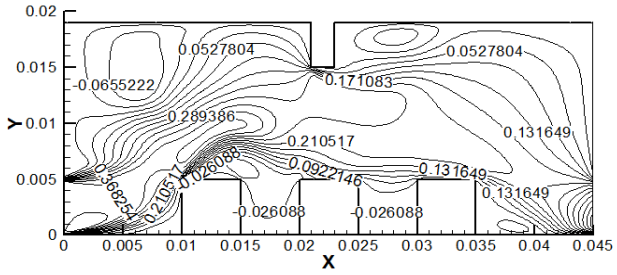

a) L/H=3.2

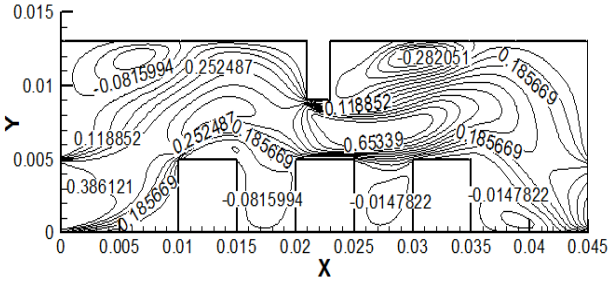

b) L/H=5.6

Fig.11 Velocity line distribution variation with Reynolds number at Ra= 8.7×10⁶ and Ri=1.3, h/H=0.2 and b/H=0.4.

Also, increasing the aspect ratio L/H will lead to disappear the cell recirculation between the heated blocks. The effect of increasing the aspect ratio L/H on the isotherm contours illustrated in **Fig.12,** the figure shoed that the isotherm contours become more separate when increasing the cavity aspect ratio.

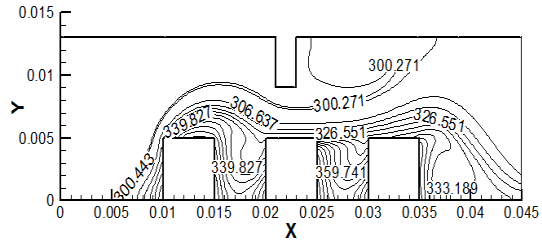

a) L/H=5.6

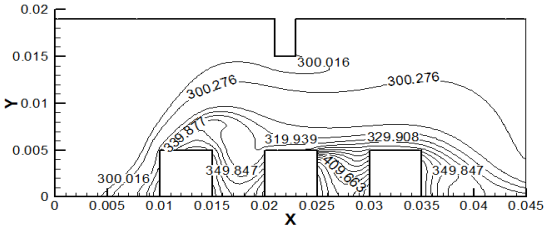

b) L/H=3.2

Fig.12 Temperatures line distribution variation with Reynolds number at Ra= 8.7×10^6 and Ri=1.3, h/H=0.2 and b/H=0.4.

The big circulation cell of the airflow velocity behind the baffle will separate into several small cells when increasing the block height ratio as presented in **Fig.13** due to decreasing the air pressure and the circulated the air behind the baffle.

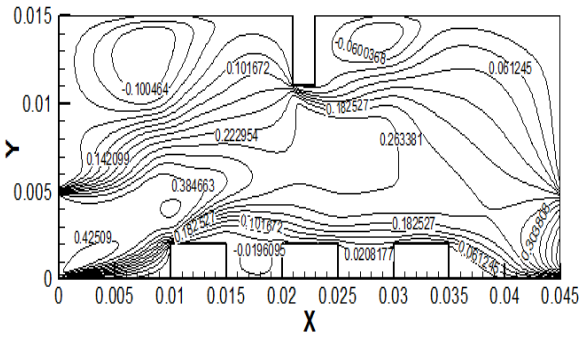

a) b/H=0.25

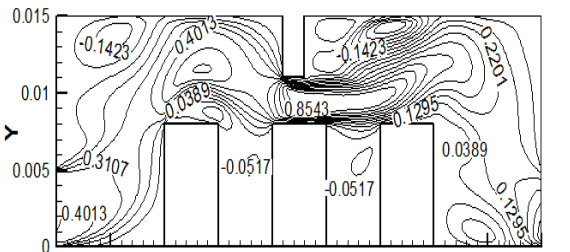

b) b/H=0.61

Fig.13: Velocity line distribution variation with Reynolds number at Ra= 8.7×10^6 and Ri=1.3, L/H=4.5 and h/H=0.2

In the same time, there is no velocity cell between the heated blocks when increasing the blocks height, due to the air velocity decreasing in this region. The effect of blocks height on the isotherm contours plotted in **Fig.14**.

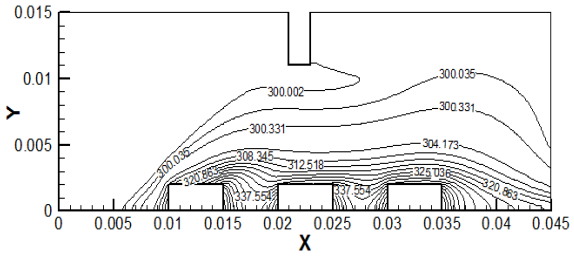

a) b/H=0.25

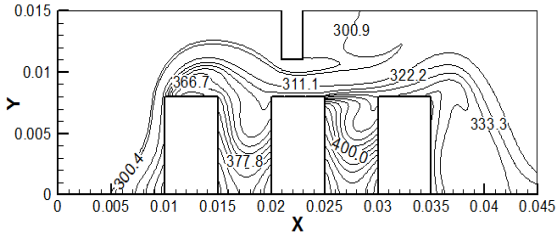

a) b/H=0.61

Fig.14 Temperatures line distribution variation with Reynolds number at Ra= 8.7×10^6 and Ri=1.3, L/H=4.5 and h/H=0.2.

The results showed that the temperatures under the baffle and in

the zones between the heated blocks increased with increasing the blocks heights increasing the Reynolds number.

Figs.15 to 18 showed the effect of Reynolds number, Richardson number, baffle height ratio, and blocks height ratio on the just outlet temperatures in the position of x=40 mm against the dimensionless cavity height y/H. The results indicated that the trend of the outlet temperature will appear same in all conditions, it increased from the upper wall of the cavity at y/H=1 to the lower wall of the cavity at y/H=0 where the heat flux was applied. However, increasing the Reynolds number will decrease the outlet temperatures at specified cavity height as plotted in **Fig.15**. Nevertheless, when increasing the Richardson number, show that the outlet temperatures will increase due to increasing the applied heat flux as plotted in **Fig.16**.

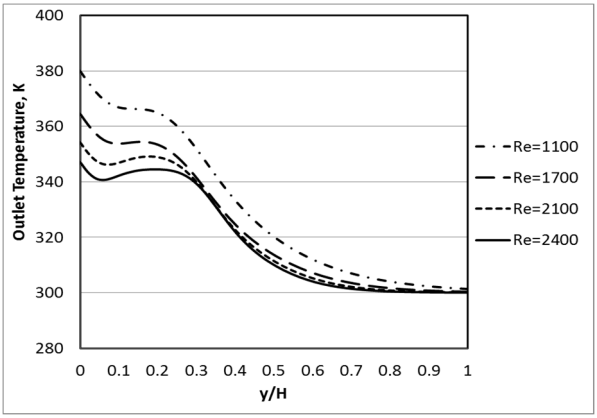

Fig.15 Variation of outlet temperatures with cavity height at Ra=8.2×10^6, Ri=8, L/H=3.2, h/H= 0.4 and b/H=0.4.

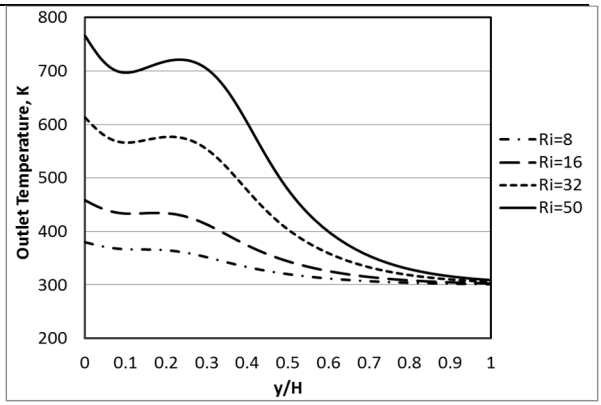

Fig.16 Variation of outlet temperatures with cavity height at Ra=8.2×10^6, Re=1100, L/H=3.2, h/H= 0.4 and b/H=0.4.

The effect of baffle height on the outlet temperatures reversed in the vertical position at y/H=0.26, due to presence the baffle in the middle of the cavity. Whereas, the outlet temperatures decrease with increasing the baffle height in the region between 0 to 0.26, but it increase with increasing the baffle height for other positions as plotted in **Fig.17**. Also, the outlet temperatures increased with increasing the blocks height as shown in **Fig.18**.

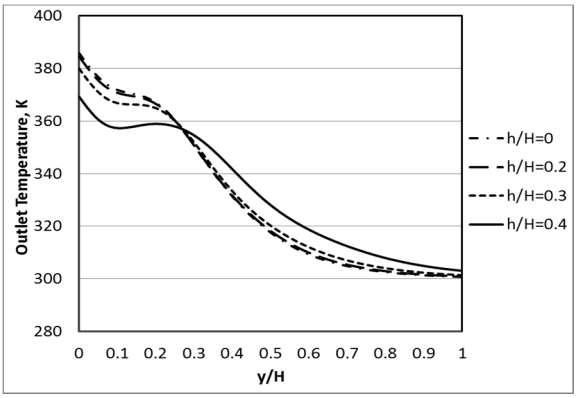

Fig.17 Variation of outlet temperatures with cavity height at Ra=8.2×10^6, Ri=8, Re=1100, L/H=3.2 and b/H=0.4.

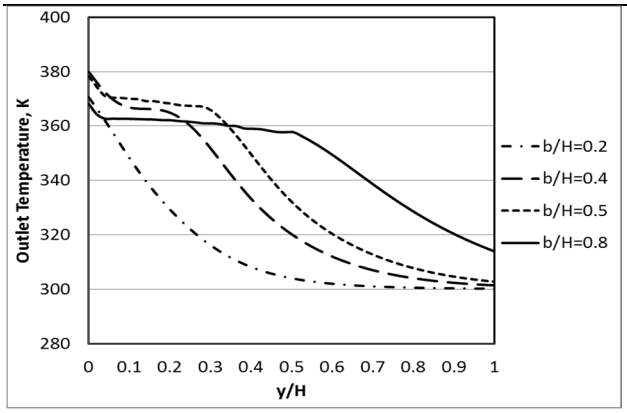

Fig.18 Variation of outlet temperatures with cavity height at Ra=8.2×10^6, Ri=8, Re=1100, L/H=3.2 and h/H= 0.4.

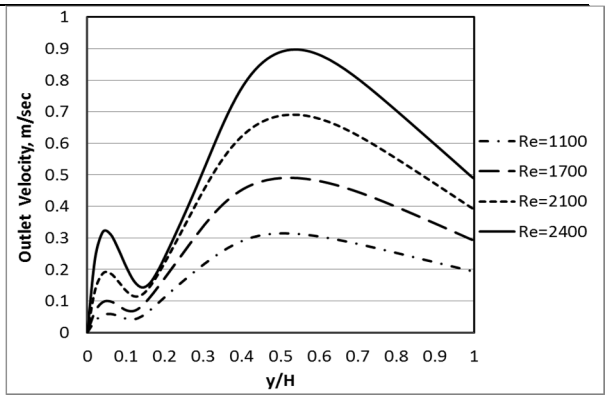

Fig.19 Variation of outlet velocity with cavity height at Ra=8.2×10^6, Ri=8, L/H=3.2, h/H= 0.4 and b/H=0.4

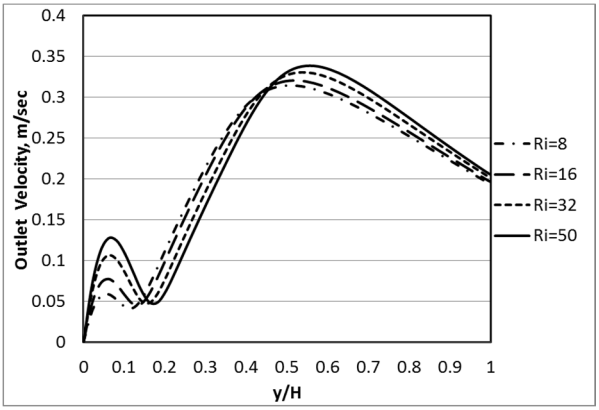

Fig.20 Variation of outlet velocity with cavity height at Ra=8.2×10^6, Re=1100, L/H=3.2, h/H= 0.4 and b/H=0.4

The effect of previous studied parameters on the just outlet velocity in the position of x=40 mm against the dimensionless cavity height y/H was given by **Figs.19 to 22**. The results showed that profile of the outlet velocity will affected by all parameters, the velocity will reflected with reversed flow near the baffle at y/H=0.14 due to the decreasing the momentum behind the baffle. However, the velocity increases with increasing Reynolds number as plotted in **Fig.19**. In addition, when increasing the Richardson number, show that the outlet velocity has two reflected points at y/H=0.16 and 0.47 as illustrated in **Fig.20**.

The outlet velocity increased with increasing the baffle height in the regions behind the baffle and blocks, due to presence the baffle in the middle of the cavity but it not affected in the region between the baffle and blocks as presented in **Fig.21**. The minimum outlet velocity was obtained when using block height ratio b/H=0.5, but, the maximum outlet velocity was obtained when using block height ratio b/H=0.8 as shown in **Fig.22**.

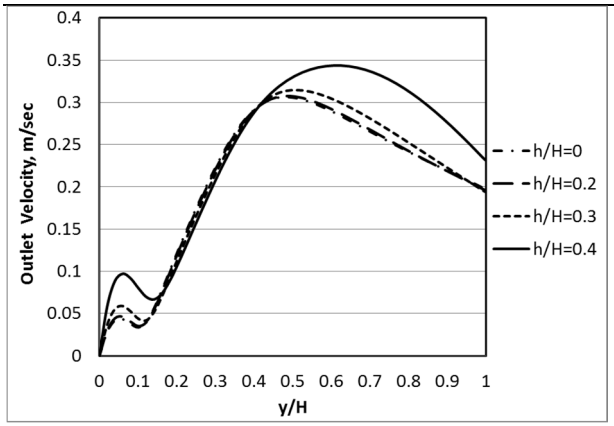

Fig.21 Variation of outlet velocity with cavity height at Ra=8.2×10⁶, Ri=8, Re=1100, L/H=3.2 and b/H=0.4

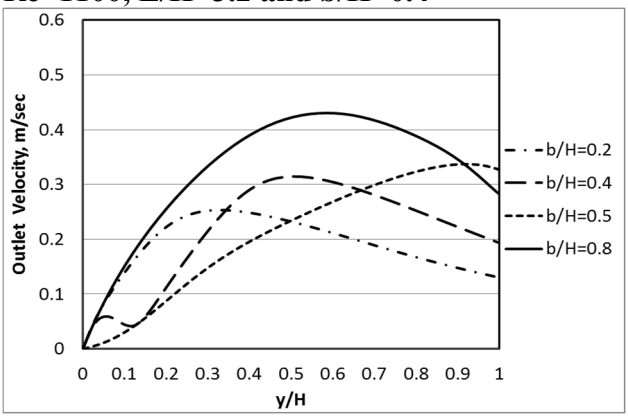

Fig.22 Variation outlet with cavity height at Ra=8.2×10⁶, Ri=8, Re=1100, L/H=3.2 and h/H= 0.4

To study the convective heat transfer inside the employed cavity, by using the effect of the Reynolds number, Richardson number, baffle height ratio, and blocks height ratio on Nusselt number. **Figs.23 to 26** showed that the Nusselt number increases by 40 % with increasing the Re from 1100 to 2400. Also, it increases by 22% when increasing the baffle height ratio h/H from 0 to 0.4, and it increased by 60% when increasing the block height ratio b/H from 0.2 to 0.8, due to decreasing the air temperatures near the blocks. Nevertheless, it decreased by -29% when increasing the block height ratio L/H 3.2 to 35.6. These present given at axial distance x/L=0.5.

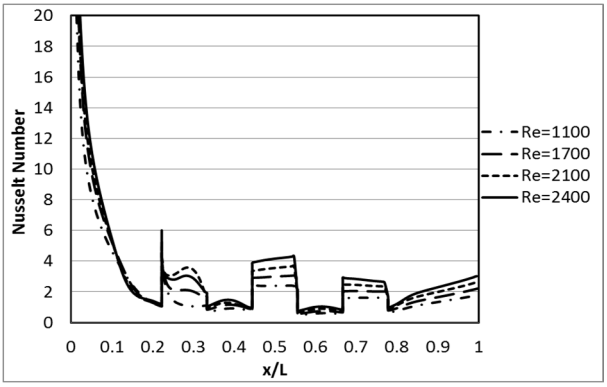

Fig.23 Variation of Nusselt number with cavity length at Ra=8.2×10⁶, Ri=8, L/H=3.2, h/H= 0.4 and b/H=0.4

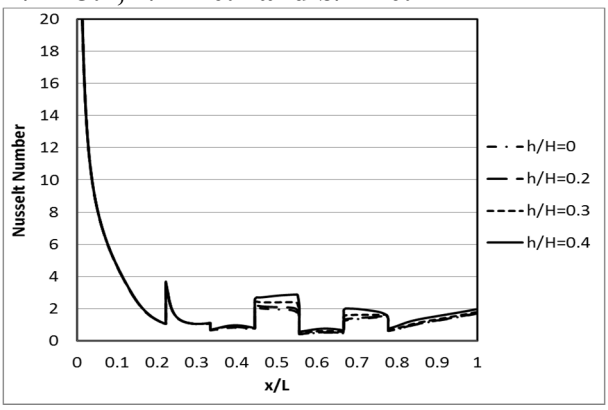

Fig.24 Variation of Nusselt number with cavity length at Ra=8.2×10⁶, Ri=8, Re=1100, L/H =3.2 and b/H=0.4

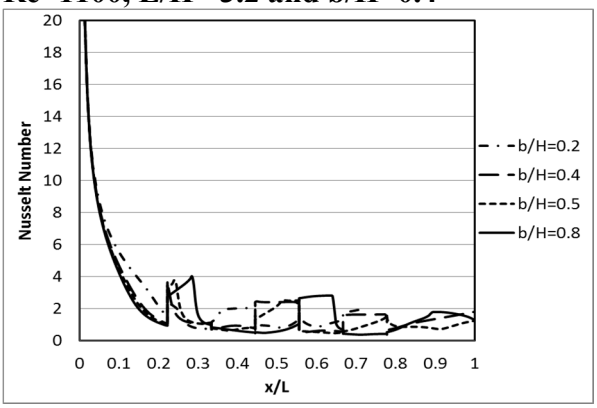

Fig.25 Variation of Nusselt number with cavity length at Ra=8.2×10⁶, Ri=8, Re=1100, L/H=3.2 and h/H= 0.4

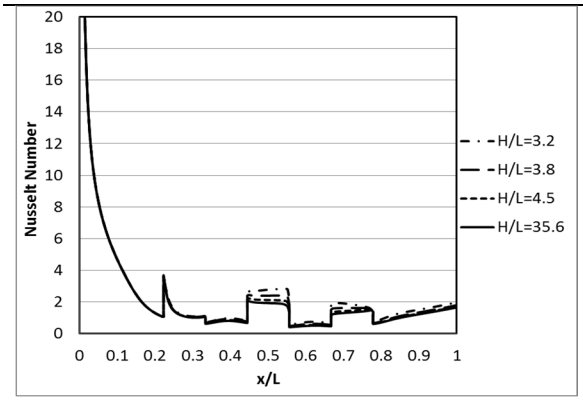

Fig.26 Variation of Nusselt number with cavity length at Ra=8.2×10^6, Ri=8, Re=1100, L/H=3.2 and b/H= 0.4

Finally, the average Nusselt number plotted with Reynolds number for different baffle height ratio h/H plotted in **Fig.27** and for different baffle height ratio h/H plotted in **Fig.28.**

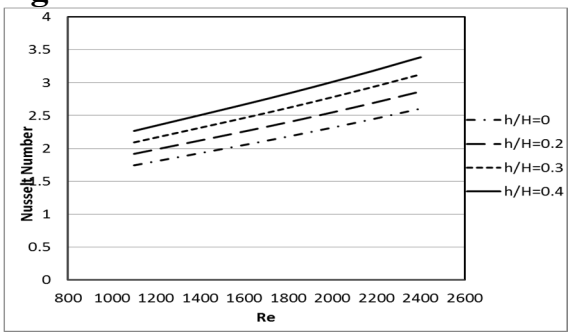

Fig.26 Average Nusselt number against Reynolds number at Ra=8.2×10^6, Ri=8, L/H=3.2 and b/H=0.4

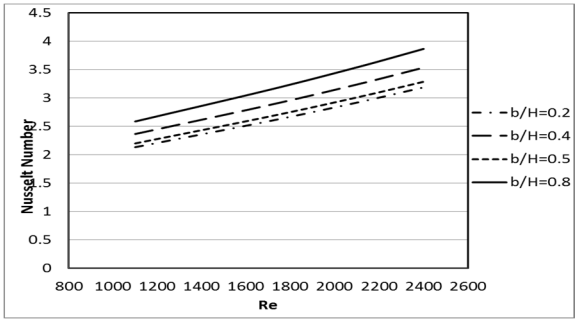

Fig.28 Average Nusselt number against the Reynolds number at Ra=8.2×10^6, Ri=8, L/H=3.2 and h/H= 0.4

Conclusions

A study of laminar forced convective heat transfer in a 2D rectangular cavity with vertical baffle and variable heights blocks was presented numerically in this study. The results give the following conclusions:

1) With increasing the Raleigh number, the Nusselt numbers increases, and with increasing the inlet Reynolds number for all cases.
2) Remarkable improvement of the cavity flow and laminar convective heat transfer is achieved by increasing baffle and blocks height from the heated bottom wall.
3) Increasing the baffle and blocks height will lead to vary the positions of the mean flow the heat transfer in the cavity.
4) Changing the cavity shape by varying its aspect ratio to change the cavity area will lead to decreasing the average Nusselt number.
5) The influence of the baffle and blocks height ratios is clearly much bigger than the influence of the cavity aspect ratio on the Nusselt number for all cases.

Nomenclatures

H height of the cavity, [m]
L length of the cavity, [m]
h height of baffle, [m]
b height of blocks, [m]
T dimensional temperature [K]
h convective heat transfer coefficient, W/m^2.K.

Nu average Nusselt number, $Nu = hd/k$.
u, v velocity components, [ms^{-1}]
U, V dimensionless velocity components
p pressure [Nm^{-2}]
P dimensionless pressure
k thermal conductivity of fluid [Wm^{-1}K^{-1}]
Pr Prandtl number, $Pr = v/\alpha$.
q" heat flux, W/m^2.
Ra Rayleigh number, $Ra = g\beta\Delta TW^3/\alpha v$.
Ri Richardson number, $Ra = Gr/Re^2$.
Re Reynolds number, $Re = u_i E/v$.
T temperature, [K]
x, y Cartesian coordinates [m]
X, Y dimensionless Cartesian coordinates
cp specific heat of the fluid, [kj/kg.K].
g gravitational acceleration [ms^{-2}]
a_E, a_W, a_N, a_S Coefficient in general finite-volume equation
A_e, A_w, A_n, A_s Area of finite-domain cell boundaries, [m^2]
F_e, F_w, F_n, F_s Convection terms

Greek Letters

α fluid thermal diffusivity, [m^2/sec].
β fluid compressibility, [K^{-1}].
μ fluid dynamic viscosity, [Pa.sec].
ν fluid kinematic viscosity, [m^2/sec].
θ dimensionless temperature
ρ density of the air, [kg/m^3].
ξ computed field variables.

Subscript

e, w, n, s Control volume faces
P, E, W, N, S Central node and its neighbors

References

[6] Ahammad, M., M., Rahman, M., Rahman , 2014, A Study On The Governing Parameters Of MHD Mixed Convection Problem in A Ventilated Cavity Containing A Centered Square Block, International Journal of Scientific & Technology Research Volume 3, ISSUE 5, pp.232-239.

[8] Bejan, A., 1993, Heat Transfer, John Wiley and Sons, pp.425.

[1] Cong R, X, Machado B., Das, 2016, Mixed Convection Flow of Nanofluid in a Square Cavity with an Intruded Rectangular Fin. International Conference on Mechanical Engineering (ICME 2015), Dhaka, Bangladesh: AIP Publishing, pp.21-32

[10] Davis, G., 1983, Natural convection of air in a square cavity, a benchmark numerical solution, Int. J. Numer., Meth., Fluid. 3, pp. 249–264.

[4] Islam, A., M., Sharif, E., Carlson, 2012, Mixed convection in a lid driven square cavity with an isothermally heated square blockage inside, Int. J. Heat Mass Transf. 55, pp.5244–5255.

[2] Oztop, H., I., Dagtekin, A., Bahloul, 2004, Comparison of position of a heated thin plate located in a cavity for natural convection, Int. Commun. Heat Mass Transfer 31, pp. 121-132.

[7] Patankar, S. V., " Numerical Heat Transfer and Fluid Flow ", 1980, Hemisphere Publishing Corporation, New York.

[3] Silva, A., É., Fontana, V., Mariani, F., Marcondes, 2010, Natural Convection Within Trapezoidal Cavity With Two Baffles On The Lower Horizontal Surface, Proceedings of ENCIT 2010 13th Brazilian Congress of Thermal Sciences and Engineering, Uberlandia, MG, Brazil, pp.215-221

[5] Silva, A., E., Fontana, V., Mariani, F., Marcondes, 2012, Numerical investigation of several physical and geometric parameters in the natural convection into trapezoidal cavities, International Journal of Heat and Mass Transfer 55, pp.6808–6818.

[9] Spalding, D.B., 1972, A novel finite difference formulation for differential expressions involving both first and second derivatives, Int. J. Numer. Methods Eng. 4, 551–559.

انتقال الحرارة بالحمل الطباقي القسري داخل مغلف مزود بحاجز مع ثلاثة صناديق مسخنة وعارضة

فارس علي بديوي
مدرس مساعد
قسم تقنيات ميكانيك القدرة
معهد تكنولوجيا -بغداد
الجامعة التقنية الوسطى
بغداد
العراق

الخلاصة

تم استخدام دراسة عددية في استقصاء انتقال الحرارة بالحمل الطباقي القسري في مغلف مستطيل مع ثلاثة صناديق مسخنة بفيض حراري ثابت مثبتة في السطح السفلي اما السطح العلوي مزود بعارضة متغيرة الارتفاع. وتم استخدام نموذج ثنائي البعد بفرض ان الجريان هو مستقر ولاأنضغاطي وطباقي. وتم حل المعادلات الحاكمة بطريقة الحجوم المحددة مع استخدام صيغة SIMPLE بترتيب التجميع للنقاط. ان التحليل العددي تم تقديمه باستخدام قيم مختلفة لنسبة الشكل للمغلف (L/H) وتتضمن (3.2, 3.8, 4.5, 5.6) وقيم مختلفة من قيم نسبة ارتفاع العارضة (h/H) وتشمل (0, 0.2, 0.3, 0.4) وايضا قيم مختلفة من نسبة ارتفاع الصناديق (b/H) وتضم (0.2, 0.4, 0.5, 0.8). وان الهواء الداخل للمغلف كان عند قيم مختلفة لعدد رالي (8.2×10^6 to 4.9×10^7) وقيم مختلفة لعدد ريكاردسون (1.3, 2.1, 3.6, 8.2) ولدراسة تاثير الحمل القسري تم استخدام هواء داخل بعدد رينولدز (1100, 1170, 1900, 2100). تم عرض النتائج باستخدام سرع الهواء ودرجات الحرارة واعداد نسلت. اظهرت النتائج ان توزيع السرع ودرجات حرارة الهواء تتأثر بشكل كبير بالجريان وشكل المغلف. وكذلك فقد تم ملاحظة ان اعداد نسلت تزداد مع زيادة اعداد رينولدز وزيادة نسب ارتفاع العارضة وزيادة نسبة ارتفاع الصناديق ولكن عدد نسلت يقل مع زيادة نسبة الشكل للمغلف في جميع الظروف المدروسة.

الكلمات المفتاحية: عارضة، صناديق مسخنة، حمل قسري طباقي، مغلف.